HAYATI
Journal of Biosciences

Vol. 33 No. 6, November 2026 1627-1636
DOI:10.4308/hjb.33.6.1627-1636
ISSN: 1978-3019
EISSN: 2086-4094

Research Article

Check for updates

OPEN ACCESS

Genetic Stability and Agronomic Performance of Transgenic Potato (*Solanum tuberosum* L.) cv. IPB CP1 Overexpressing *FBPase* and *ClRan1* Genes Across Three Generations

Redi Fajar Kurniawan[1], Aris Tjahjoleksono[2,3*], Miftahudin[2,3]

[1]*Biotechnology Graduate Program, Graduate School, IPB University, Bogor 16680, Indonesia*
[2]*Department of Biology, Faculty of Mathematics and Natural Science, IPB University, Bogor 16680, Indonesia*
[3]*Biotech Center, International Research Institute for Advanced Technology, IPB University, Bogor 16680, Indonesia*

ARTICLE INFO

Article history:
Received December 22, 2025
Received in revised form June 19, 2026
Accepted October 12, 2026
Available Online November 2, 2026

KEYWORDS:
ClRan1,
FBPase,
IPB CP1,
potato,
productivity,
superior variety

Copyright (c) 2026 @author(s).

ABSTRACT

Potato (*Solanum tuberosum* L.) is an essential crop in Indonesia, yet domestic productivity continues to lag behind rising consumption. The *FBPase* gene encodes the FBPase enzyme involved in sucrose biosynthesis, whereas the *ClRan1* gene regulates mitotic cell division; co-expressing these genes offers a promising strategy to enhance yield potential. This study evaluated the genetic stability, gene expression, physiological and morphological responses, as well as yield performance of transgenic IPB CP1 potatoes overexpressing *FBPase* and *ClRan1* genes across three generations (G_0, G_1, and G_2). Using a randomized complete block design, four transgenic clones (C1FB1–C1FB4) were evaluated alongside a non-transgenic control. Transgene integration was verified by PCR, transcript expression was quantified by RT-qPCR, and photosynthetic parameters, including photosynthetic rate, stomatal conductance, and intercellular CO_2 concentration, were measured using a LI-COR LI-6400XT system. PCR analysis confirmed the stable integration of both transgenes in all transgenic clones across all generations. Gene expression was detected in all generations, stabilizing in G_1 and G_2 following transient silencing in G_0. Transgenic clones exhibited significantly higher photosynthetic rates and stomatal conductance, accompanied by increased root length and total biomass. Consequently, tuber weight and number were significantly greater in G_1 and G_2 relative to the non-transgenic control. These findings demonstrate that the combined overexpression of *FBPase* and *ClRan1* in IPB CP1 potato enhanced physiological efficiency and yield potential. Among the evaluated lines, clone C1FB4 showed the highest transgene expression level and superior agronomic performance, highlighting its promise as a candidate line for improving national potato productivity.

1. Introduction

Potato (*Solanum tuberosum* L.) is the world's third most consumed commodity (Eed *et al*. 2025). Despite a 4.13% annual increase in domestic potato production from 2018 to 2022, Indonesian potato consumption grew at a much faster rate of 12.28% per year. Indonesia currently addresses this domestic supply gap through imports (Maulidiyah *et al*. 2025). However, relying on imports is not a sustainable long-term solution, as domestic market prices remain vulnerable to exchange rate volatility and global supply chain disruptions

*Corresponding Author
E-mail Address: aristj@apps.ipb.ac.id

(Baranauskaitė and Jurevičienė 2021). Consequently, the application of genetic engineering offers a strategic approach to overcome these domestic productivity constraints.

Genetic engineering enables the precise introduction or modification of specific traits to develop crop cultivars with superior agronomic performance (Kalendar *et al*. 2022; Musawira *et al*. 2025). Transgenic plants can increase yields by approximately 13-100% (Song and Han 2021). Among the genetic engineering strategies used by researchers, *Agrobacterium*-mediated transformation is widely used (Niedbała *et al*. 2021). Olivah (2019) successfully transformed the IPB CP1 potato cultivar with the *FBPase* and *ClRan1* genes via *Agrobacterium tumefaciens*. The *FBPase* gene encodes fructose-1,6-bisphosphatase, a key enzyme regulating sucrose and starch biosynthesis (Tian *et al*. 2025). Meanwhile, the *ClRan1* gene encodes a small GTP-binding protein (RAN) essential for mitotic cell division and nucleocytoplasmic transport (Xu and Cai 2014).

The *FBPase* gene was originally isolated from cyanobacteria, whereas *ClRan1* was derived from *Citrullus lanatus*. Expressing these genes in potato has been shown to enhance tuber production. Notably, simultaneous expression of both genes yields a significantly greater increase in tuber production than expressing either gene individually (Yokota *et al*. 2013), demonstrating the synergistic potential of this dual-gene strategy in cultivar IPB CP1. Building on this foundation, Olivah (2019) successfully transformed the IPB CP1 potato via *Agrobacterium*-mediated transformation, yielding four transgenic lines expressing both genes in the clonal G_0 generation. However, the stability and expression of the *FBPase* and *ClRan1* genes, and how their expression affects the physiological, morphological, and yield characteristics across subsequent generations, have not yet been evaluated. Therefore, this study aimed to evaluate the genetic stability and gene expression levels, along with the physiological, morphological, and yield performance of the transgenic IPB CP1 potato clones across three generations (G_0, G_1, and G_2) under greenhouse conditions.

2. Materials and Methods

2.1. Plant Materials and Treatments

The experiment was arranged in a randomized complete block design (RCBD) (Putra *et al*. 2019) with plant genotype (transgenic and non-transgenic) as the single factor. The plant materials comprised four transgenic clones (C1FB1, C1FB2, C1FB3, and C1FB4) and one non-transgenic control clone (C1NT), all originating from the transformation study by Olivah (2019). The experiment included five replications, with each experimental unit consisting of five plants per clone (25 plants per block). All plants were cultivated in a greenhouse under standard agronomic management. Irrigation was provided at 500 mL of water per plant every two days. Fertilization consisted of weekly applications of 250 mL of 5 g/L liquid NPK fertilizer per plant. Pest and disease control were maintained by weekly sprays of abamectin (0.5-1.0 mL/L) and mancozeb (2.0-3.0 g/L), supplemented with biweekly applications of difenoconazole (0.5-1.0 mL/L).

Plantlets of the non-transgenic and transgenic clones were acclimatized in the greenhouse for two weeks before transfer to seedling trays containing cocopeat for an additional two weeks. Subsequently, plants were transplanted into 30 cm polybags filled with a mixture of cocopeat and fermented manure, where they were grown until harvesting the G_0 tubers. These harvested tubers served as seed material for the subsequent G_1 and G_2 generations.

2.2. Transgene Integration Analysis

Genomic DNA was extracted from young leaf tissue of IPB CP1 potato plants using the Plant Genomic DNA Mini Kit (Geneaid, Taiwan). DNA concentration and purity were measured using a nano-spectrophotometer (Maestro, Taiwan), and DNA integrity was verified by 1% (w/v) agarose gel electrophoresis in 1 × TAE buffer at 100V for 30 minutes (Optima, Japan). High-quality DNA samples were used for PCR amplification to confirm the integration of *FBPase* and *ClRan1*. PCR analysis was performed using gene-specific primers (*FBPase* and *ClRan1*), with the *actin* gene serving as an internal control to ensure template consistency (Table 1). The primer sequences used in this study were adopted from Olivah (2019).

PCR was performed in 10 µL reaction volumes containing 1.0 µL of template DNA, 0.25 µL of forward primer, 0.25 µL of reverse primer, 5.0 µL of DreamTaq Green PCR Master Mix, and 3.5 µL of nuclease-free water. The thermal cycling conditions consisted of an initial denaturation at 95°C for 5 minutes, 35 cycles of denaturation at 95°C for 30 seconds, annealing at 60°C for 45 seconds, and extension at 72°C for 1 minute. Following the completion of the cycle, a final extension step at 72°C for 5 minutes was performed. PCR amplicons were resolved on a 1% agarose gel electrophoresis in

1×TAE buffer at 100V for 28 minutes. A 1 kb KAPATM Universal Ladder (Kapabiosystem, USA) was used as a molecular weight standard. The resulting DNA bands were visualized under UV transillumination and documented using a Gel-Doc system.

2.3. Transgene Expression Analysis

Transgene expression was quantified using reverse transcription quantitative PCR (RT-qPCR). Total RNA was extracted from 50 mg of leaf tissue using the Total Plant RNA Mini Kit (Geneaid, Taiwan). Purified RNA was reverse transcribed into cDNA using the ReverTra Ace® qPCR RT Master Mix with gDNA Remover (Toyobo, Japan). The resulting cDNA was used to determine the transcript levels of *FBPase* and *ClRan1*, with *actin* as the internal reference gene (Table 2). Each qPCR reaction (10 µL) contained 1.0 µL of cDNA template (50 ng), 5.0 µL of ThunderbirdTM SYBR® qPCR Mix, 0.25 µL of forward primer (0.3 µM), 0.25 µL of reverse primer (0.3 µM), and 3.5 µL of nuclease-free water. The qPCR was conducted on a QuantStudio 5 Real-Time PCR System (Thermo Scientific, USA). Thermal cycling parameters consisted of initial enzyme activation at 95°C for 5 seconds; 55 cycles of denaturation at 95°C for 5 seconds, annealing at 58°C for 10 seconds, and extension at 72°C for 10 seconds. Relative gene expression was calculated using the $2^{-\Delta\Delta C_T}$ method (Livak and Schmittgen 2001).

Table 1. Primer sequences used for integration analysis

Gene	Primer	Primer sequence
Actin	acT-F	ATGGCAGATGCCGAG-GATAT
	acT-R	CAGTTGTGCGACCACTT-GCA
FBPase	rbcS-F	TGAGATAAGGACGAGT-GAGG
	FBPase_65R	TGCCCACTTCTTCACC-GATA
ClRan1	35S-F1	AAACCTCCTCGGATTC-CATT
	CLRAN1-genome-04r	TGTGGAATGTGACTT-GCTTGGC

Table 2. Primer sequences used for gene expression analysis

Gene	Primer	Primer sequence
Actin	Tact-qF	ACATCGTCCTTAGTG-GTGGA
	Tact-qR	GTGGACAATGGAAGG ACCAG
FBPase	FBPase-SKqF	GTCCGTCTGATCAGC-GATG
	FBPase-SKqR	TAGATCAGCTGGCCTTG-GAAG
ClRan1	ClRan1-qF	GCAAGTCACATTCCA-CAGGA
	ClRan1-qR	G A A G A G G T T G A C T TGCTGCT

2.4. Physiological Characteristics

Photosynthetic parameters were measured using a LI-COR LI-6400XT portable photosynthesis system (LI-COR, USA). Evaluated parameters included the photosynthetic rate (*A*), stomatal conductance (*gs*), and intercellular CO_2 concentration (*Ci*). Measurements were taken on fully expanded young leaves at 6 weeks after planting (WAP) according to Guo *et al*. (2025). To minimize environmental fluctuation, all measurements were conducted between 09:00 and 12:30 in five replications.

2.5. Morphological Characteristics and Tuber Yield

Morphological and yield parameters were evaluated across all three generations (G_0, G_1, and G_2). Vegetative growth parameters, including plant height, root length, shoot dry mass, and root dry mass, were measured during the late vegetative phase (6-7 WAP). Root-to-shoot ratios were calculated based on dry mass. Yield components, specifically fresh tuber number per plant and fresh tuber weight per plant, were determined at harvest (12-14 WAP).

2.6. Data Analysis

Data were subjected to one-way analysis of variance (ANOVA) using SAS software (version 9.0). Significant differences among clone means were identified using Duncan's Multiple Range Test (DMRT) at α=0.05.

3. Results

3.1. Integration of *FBPase* and *ClRan1* Transgenes Across Three Generations

Electrophoresis confirmed the presence of the target transgenes (*FBPase* and *ClRan1*) across the G_0, G_1, and G_2 generations of transgenic IPB CP1 potato clones (Figure 1). PCR amplification produced distinct DNA fragments corresponding to the expected sizes for each gene: approximately 580 bp for *FBPase* and 800 bp for *ClRan1* (Figure 1B-C). Amplification of the *actin* gene (746 bp) served as the internal control for genomic DNA quality and was consistently detected across all transgenic clones and the non-transgenic control (C1NT)

(Figure 1A). No transgene bands (*FBPase* or *ClRan1*) were detected in the non-transgenic control clone C1NT, confirming the specific integration of both constructs in transgenic lines C1FB1 through C1FB4 across all three evaluated generations.

3.2. Relative Expression Analysis of *FBPase* and *ClRan1* Transcripts

Quantitative real-time PCR (RT-qPCR) was performed to evaluate target transcript expression in leaf tissue, normalized against the internal reference gene (*actin*). Basal transcript levels of endogenous *FBPase* and *ClRan1* were detected in the non-transgenic control clone (C1NT) across all generations (G_0, G_1, and G_2) and set as the baseline calibrator (1.0-fold expression) (Figure 2).

All transgenic clones exhibited marked overexpression of both *FBPase* and *ClRan1* relative to C1NT across all generations, though transcript levels varied among specific clones and generational cohorts (Figure 2). In the G_0 generation, clone C1FB2 displayed the lowest initial relative expression of both *FBPase* and *ClRan1*, which subsequently increased in G_1 and G_2 (Figure 2). In contrast, clone C1FB4 consistently exhibited the highest transcript abundance for both target genes across all three generations (reaching approximately 11.5-fold for *ClRan1* and 4.5-fold for *FBPase* in G_0, 6.2-fold for both genes in G_1, and 8.2-fold for *ClRan1* and 11.0-fold for *FBPase* in G_2) (Figure 2). These results demonstrate active and stable transgenerational transcription of both integrated cassettes.

3.3. Physiological Responses to Transgene Overexpression

Physiological analysis using the Li-6400 XT system revealed significant differences between transgenic and non-transgenic clones in photosynthetic rate (*A*), stomatal conductance (*gs*), and intercellular CO_2 concentration (*Ci*) (Table 3). Transgenic clones consistently exhibited higher photosynthetic rates across all generations. Stomatal conductance was significantly higher in transgenic clones during G_0 and G_2, whereas no significant difference was observed in G_1. Among the transgenic clones, C1FB4 consistently showed the highest photosynthetic rate, intercellular CO_2 concentration, and stomatal conductance across all generations. In G_0, its photosynthetic rate was not significantly different from those of C1FB1 and C1FB3; however, in G_1 and G_2, C1FB4 was significantly higher than all other clones. For stomatal conductance, C1FB4 and C1FB3 did not differ significantly, although C1FB4 maintained higher numerical values. Overall, C1FB4 exhibited the strongest physiological enhancements, mirroring its high transcript expression levels of *FBPase* and *ClRan1*.

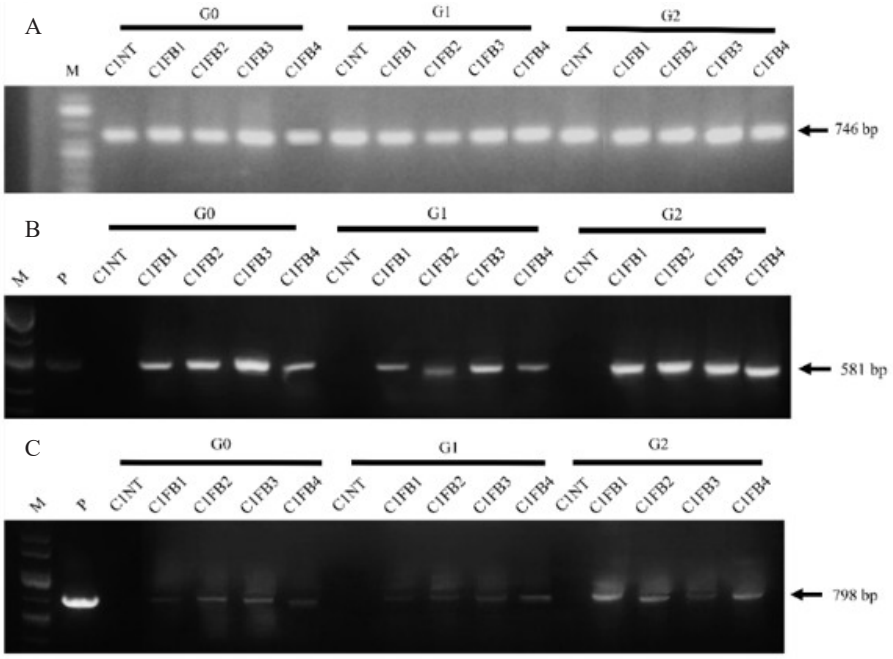


Figure 1. (A) Electrophoregrams of the *actin*, (B) *FBPase*, and (C) *ClRan1* genes in IPB CP1 potato plants across three generations. M: KAPATM Universal Ladder, P: plasmid (positive control), C1NT: non-transgenic clone, C1FB1-4: transgenic clones, G_0: generation 0, G_1: generation 1, G_2: generation 2, and bp: base pairs

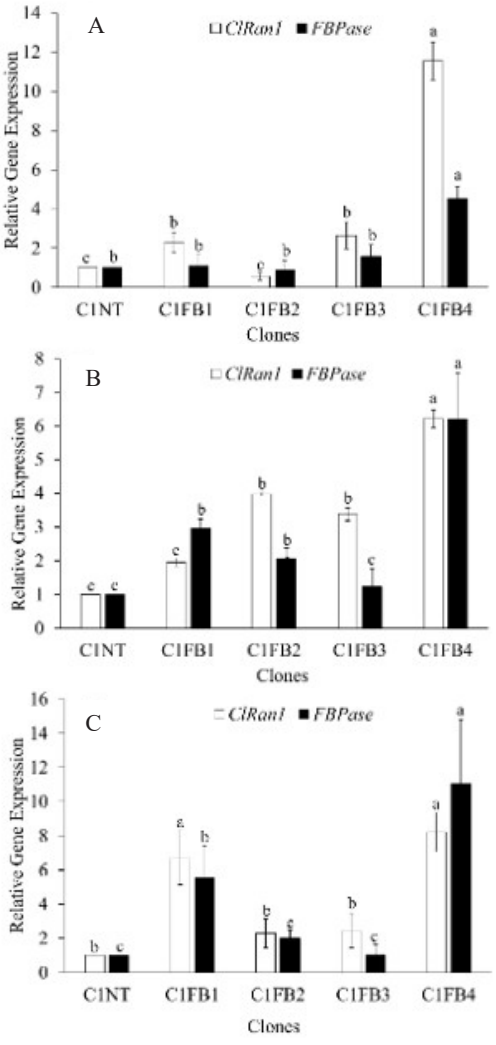


Figure 2. (A) Relative expression levels of the *FBPase* and *ClRan1* genes in IPB CP1 potato plants across generation 0, (B) generation 1, and (C) generation 2. Relative expression was calculated using the $2^{-\Delta\Delta C_T}$ method with *actin* as the internal reference gene. The non-transgenic control clone (C1NT) was designated as the baseline calibrator (relative expression = 1.0) to determine fold-overexpression in transgenic lines (C1FB1–C1FB4). Bars represent the mean ± standard error (SE) of five replicates (n=5)

3.4. Morphological Responses to Transgene Overexpression

Morphological assessment of the IPB CP1 potatoes revealed significant differences between the non-transgenic and transgenic clones (Table 4). While plant height did not differ significantly among clones in G_0, transgenic clones were significantly taller than C1NT in the G_1 and G_2 generations.

Root length also differed significantly in G_0 and G_1 (Table 4), with transgenic clones exhibiting longer roots than the non-transgenic clone (Figure 3). However, root-to-shoot dry mass ratios showed no significant differences among clones across all evaluated generations (Table 5). Among the transgenic clones, C1FB2 exhibited the shortest roots in G_0, while both C1FB1 and C1FB2 remained shorter than the other transgenic clones in subsequent generations. In contrast, C1FB4 consistently performed best, maintaining the greatest root length across all generations.

3.5. Yield Performance

Transgenic IPB CP1 clones produced significantly higher tuber numbers and total tuber weights per plant than C1NT in G_1 and G_2, whereas differences in G_0 were not statistically significant (Table 6, Figure 4). Evaluation of yield traits revealed notable variation among individual transgenic lines (Table 6). Although G_0 exhibited no significant differences, data from G_1 and G_2 demonstrated that C1FB4 consistently produced the highest tuber number, weight, and size, whereas C1FB2 recorded the lowest tuber weight among the transgenic lines. Notably, in G_2, the total tuber weight of C1FB4 was statistically similar to that of the non-transgenic control (C1NT); however, C1FB4 produced a higher quantity of tubers. Overall, C1FB4 exhibited superior yield performance across all generations.

Table 3. Photosynthetic rate, intercellular CO_2 concentrations, and stomatal conductance of IPB CP1 potato plants across three generations

Clones	A (µmol CO_2/m^2s)			Ci (µmol/mol)			*gs* (mol H_2O/m^2s)		
	G_0	G_1	G_2	G_0	G_1	G_2	G_0	G_1	G_2
C1NT	19.11±1.58^b	19.84±0.83^c	47.38±3.82^c	325.37±20.49^b	244.31±71.69^c	766.66±207.04^b	0.71±0.16^b	0.45±0.26^a	1.63±0.96^d
C1FB1	21.67±1.36^a	22.34±1.41^{ab}	54.95±4.15^b	336.87±8.88^{ab}	304.1±9.11^{abc}	1043.88±6.16^a	0.96±0.20^b	0.81±0.14^a	4.23±0.37^b
C1FB2	19.69±1.02^b	21.32±1.11^b	51.91±3.92^{bc}	325.94±7.27^b	260.33±68.89^{bc}	1009.10±19.95^a	0.90±0.09^b	0.70±0.68^a	2.82±0.46^c
C1FB3	21.76±1.30^a	22.02±1.17^b	56.28±3.13^{ab}	335.18±4.79^{ab}	315.03±37.63^{ab}	1043.63±39.56^a	1.11±0.22^{ab}	0.69±0.43^a	4.80±0.13^{ab}
C1FB4	22.49±0.32^a	23.57±0.74^a	59.89±2.49^a	348.28±6.47^a	347.28±15.49^a	1056.40± 8.31^a	1.59±0.76^a	1.29±0.41^a	5.14±0.51^a

C1NT: non-transgenic clone; C1FB1-4: transgenic clones. A: photosynthetic rate, Ci: intercellular CO_2 concentration, and *gs*: stomatal conductance. G_0: generation 0, G_1: generation 1, and G_2: generation 2. Values presented as means ± standard deviation (SD). Means within the same column followed by different letters indicate significant differences based on DMRT at α = 5%. Data represent the mean of five replicates (n=5)

Table 4. Plant height and root length of IPB CP1 potato plants across three generations

Clones	Plant height (cm)			Root length (cm)		
	G_0	G_1	G_2	G_0	G_1	G_2
C1NT	55.46±8.87^{a}	67.19±11.77^{c}	53.50±9.23^{ab}	12.37±1.74^{b}	15.83±2.39^{b}	36.95±1.74^{a}
C1FB1	61.53±6.24^{a}	72.05±6.76^{abc}	51.88±4.72^{b}	15.21±2.36^{ab}	16.04±2.17^{b}	41.15±2.36^{a}
C1FB2	51.80±6.95^{a}	70.17±8.10^{bc}	62.25±6.27^{a}	13.27±5.78^{b}	15.99±1.69^{b}	33.18±5.78^{a}
C1FB3	45.20±11.31^{a}	79.60±6.25^{ab}	54.15±4.79^{ab}	16.02±2.62^{ab}	17.49±1.92^{ab}	34.15±2.62^{a}
C1FB4	54.76±8.84^{a}	83.61±7.91^{a}	47.28±7.86^{b}	19.21±2.05^{a}	19.66±1.82^{a}	34.21±2.05^{a}

C1NT: non-transgenic clone; C1FB1-4: transgenic clones. G_0: generation 0, G_1: generation 1, and G_2: generation 2. Values presented as means ± standard deviation (SD). Means within the same column followed by different letters indicate significant differences based on DMRT at α = 5%. Data represent the mean of five replicates (*n*=5)

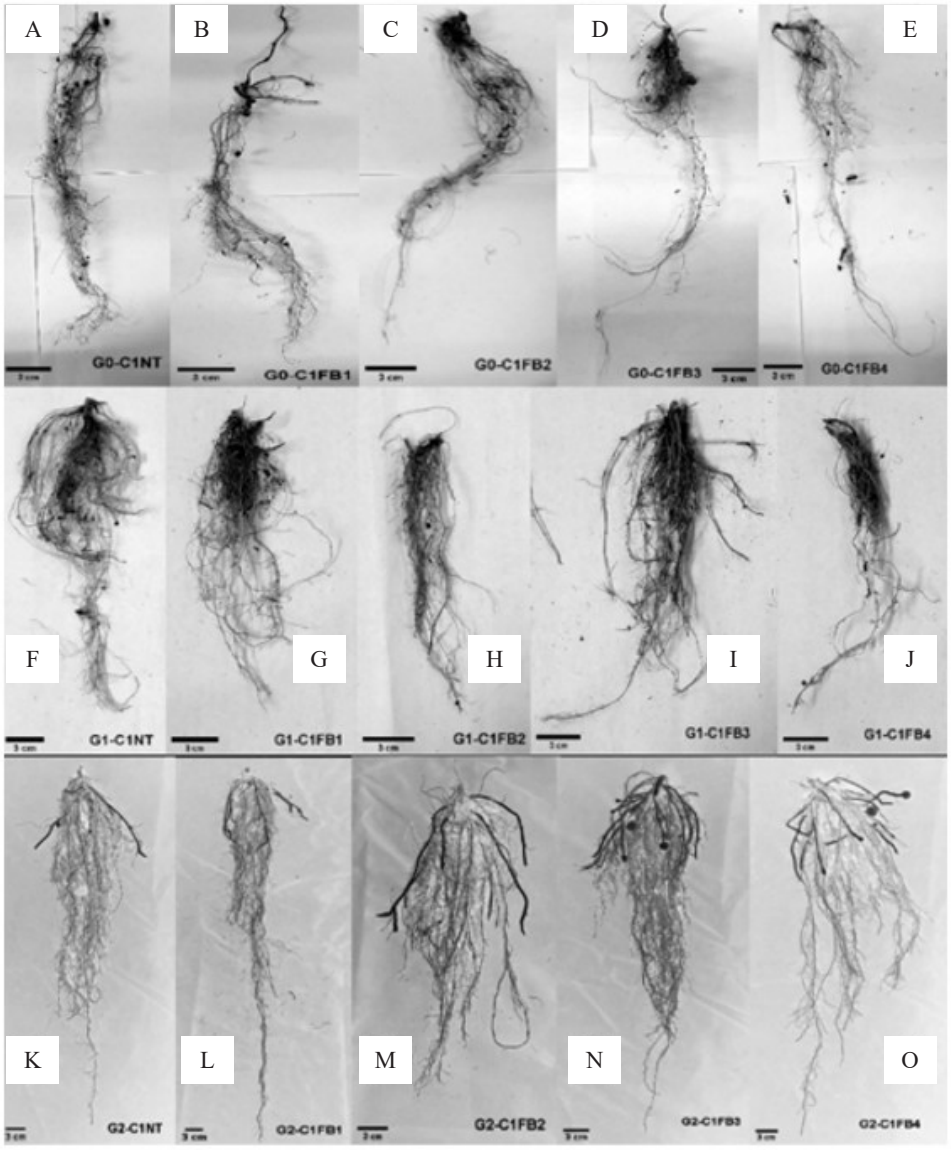


Figure 3. Root morphology of transgenic and non-transgenic IPB CP1 potato plants across three generations. (A-E): generation 0, (F-J): generation 1, and (K-O): generation 2. Scale bars = 3 cm

Table 5. Root-to-shoot ratio of IPB CP1 potato plants across three generations

Clone	Root-to-shoot ratio		
	G_0	G_1	G_2
C1NT	0.109±0.01[a]	0.031±0.02[a]	0.061±0.01[a]
C1FB1	0.102±0.03[a]	0.037±0.01[a]	0.086±0.04[a]
C1FB2	0.114±0.05[a]	0.032±0.02[a]	0.069±0.02[a]
C1FB3	0.145±0.01[a]	0.033±0.01[a]	0.132±0.06[a]
C1FB4	0.142±0.01[a]	0.038±0.01[a]	0.099±0.04[a]

C1NT: non-transgenic clone; C1FB1-4: transgenic clones. G_0: generation 0, G_1: generation 1, and G_2: generation 2. Values presented as means ± standard deviation (SD). Means within the same column followed by different letters indicate significant differences based on DMRT at α = 5%. Data represent the mean of five replicates (*n*=5)

Table 6. Number of tubers and tuber weight per plant of IPB CP1 potato clones across three generations

Clones	Tuber yields (gr/plant)			Number of tubers (tubers/plant)		
	G_0	G_1	G_2	G_0	G_1	G_2
C1NT	88.58±36.48[a]	70.53±42.42[b]	183.38±34.85[a]	10.20±1.92[b]	6.68±1.41[c]	3.00±1.00[b]
C1FB1	113.43±18.51[a]	94.83±40.60[b]	115.46±68.84[b]	14.00±1.14[ab]	7.96±1.48[abc]	4.6±1.34[ab]
C1FB2	98.60±48.94[a]	73.08±28.67[b]	47.19±18.96[c]	11.00±9.75[b]	7.33±1.63[bc]	3.40±0.55[b]
C1FB3	120.17±30.99[a]	102.91±25.24[ab]	120.17±30.99[b]	15.00±13.98[a]	9.88±2.64[ab]	4.20±1.48[ab]
C1FB4	124.42±14.27[a]	154.47±62.18[a]	185.71±26.60[a]	15.20±14.85[a]	10.36±1.88[a]	5.60±1.52[a]

C1NT: non-transgenic clone; C1FB1-4: transgenic clones. G_0: generation 0, G_1: generation 1, and G_2: generation 2. Values presented as means ± standard deviation (SD). Means within the same column followed by different letters indicate significant differences based on DMRT at α = 5%. Data represent the mean of five replicates (*n*=5)

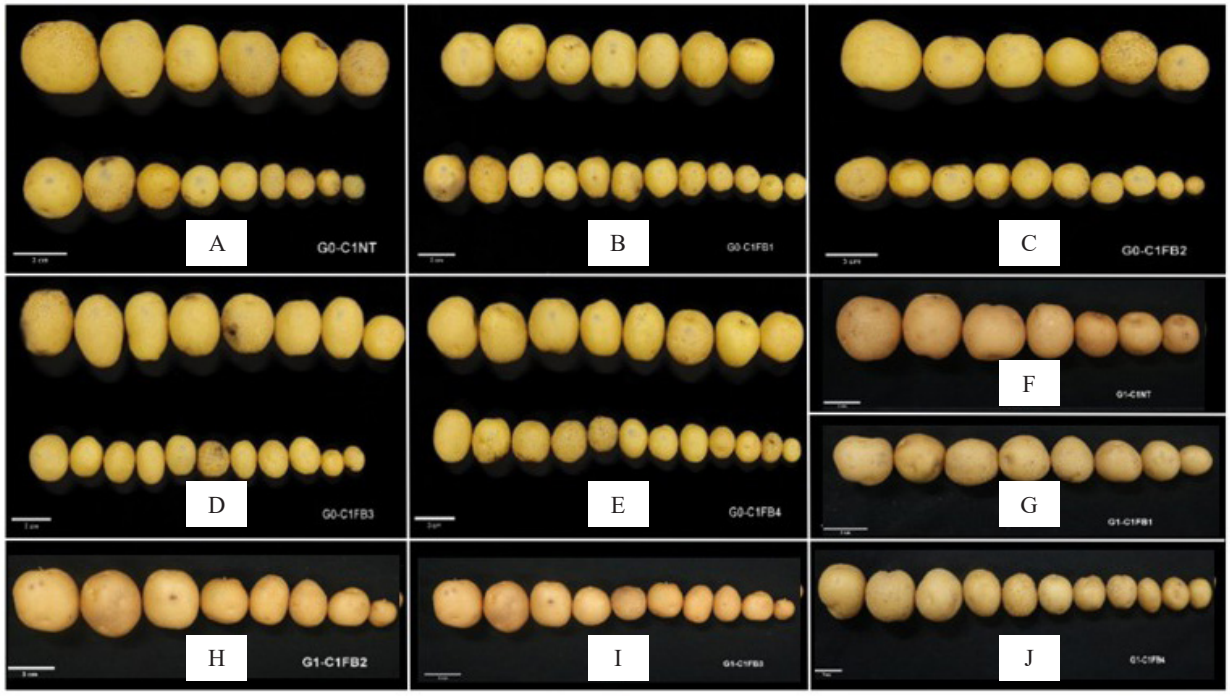


Figure 4. Tuber morphology of transgenic and non-transgenic IPB CP1 potato plant in two generations. (A-E): generation 0 and (F-J): generation 1. Scale bars = 3 cm

4. Discussion

The uniformity of *actin* amplicons across non-transgenic and transgenic lines indicates that the integration of *FBPase* and *ClRan1* did not cause major genomic rearrangements or disrupt essential housekeeping gene sequences. Housekeeping genes are standard internal references for evaluating the structural integrity of the host genome following transformation (Ruan and Lai 2007). The detection of single, expected bands for *actin*, *FBPase*, and *ClRan1* demonstrates stable integration and persistent transgenerational inheritance of the target constructs without detectable insertions or deletions (Paul *et al*. 2022; Kamian *et al*. 2023).

Sustained overexpression of *FBPase* and *ClRan1* across G_0, G_1, G_2 demonstrates that both transgenes maintained transcriptional activity; this stable expression is driven by the robust promoters used in the expression vector: the light-inducible, tissue-specific rbcS promoter controlling *FBPase*, and the constitutive CaMV 35S promoter controlling *ClRan1*. The rbcS promoter directs transgene expression primarily to chlorophyll-containing green tissues in response to light (Thanh *et al*. 2012). Overexpression of *FBPase* in leaves accelerates the conversion of fructose-1,6-bisphosphate to fructose-6-phosphate, a key metabolic node supplying precursor pools for sucrose synthesis and subsequent starch accumulation (Daie 1993; Tian *et al*. 2025). Conversely, the CaMV 35S promoter confers constitutive transcription across most plant tissues (Huang and Schiefelbein 2015), enabling ubiquitous expression of *ClRan1*. Overexpression of *ClRan1* enhances nucleocytoplasmic transport and mitotic division (Clarke and Zhang 2008), which promoted primary root elongation in transgenic clones relative to C1NT. Thus, the dual-promoter cassette successfully supported enhanced vegetative growth and carbon assimilate production without inducing deleterious pleiotropic effects.

The lower initial transcript levels observed in clone C1FB2 during G_0 likely reflect transient gene silencing, a phenomenon frequently occurring in early transgenic generations that is often reset in subsequent progeny (Andrieu *et al*. 2012). This explanation is supported by the observed recovery of *FBPase* and *ClRan1* transcript abundance in C1FB2 during G_1 and G_2.

Physiologically, overexpression of *FBPase* and *ClRan1* substantially enhanced gas exchange capacities. Transgenic clones maintained higher photosynthetic rates (*A*), stomatal conductance (*gs*), and intercellular concentration (*Ci*) values than C1NT. Increased *FBPase* expression enhances sink demand for photosynthetic intermediates, preventing metabolic feedback inhibition and sustaining higher Calvin cycle turnover (Gizak *et al*. 2019; Deng *et al*. 2021). Higher *Ci* levels indicate elevated internal CO_2 availability driven by wider stomatal apertures (*gs*), which promotes Rubisco carboxylation efficiency. Furthermore, while *ClRan1* does not directly modulate photosynthetic light reactions, its role in stimulating active cell division increases overall sink demand, which is supported by increased photosynthetic carbohydrate production (Ezaki *et al*. 2024).

The absence of significant differences in stomatal conductance (*gs*) during G_1 contrasts with the trends in G_0 and G_2. This variation may reflect endogenous fluctuations in abscisic acid (ABA) signaling, which dynamically controls stomatal closure in response to subtle microclimatic variations during plant growth (Hsu *et al*. 2021; Wei *et al*. 2025). Increased ABA accumulation in G_1 may have reduced stomatal opening, potentially due to environmental stress conditions that trigger stomatal closure to minimize water loss or prevent pathogen entry (Dodd 2013; Wei *et al*. 2025).

Morphologically, the lack of significant differences in plant height during G_0 may also be linked to early developmental lag or transient silencing effects (Andrieu *et al*. 2012). In contrast, marked increases in plant height in G_1 and G_2 reflect the synergistic actions of *FBPase* (providing carbon skeletons) and *ClRan1* (driving cellular expansion and division). Enhanced root length in transgenic lines directly aligns with the function of *ClRan1* in promoting root apical meristem mitosis (Akashi *et al*. 2016). Although enhanced root elongation was observed, root-to-shoot dry mass ratios remained unchanged among clones, indicating that photoassimilates were preferentially allocated toward tuber sink organs rather than disproportionately altering shoot-to-root structural biomass partitioning.

Yield component analysis confirmed that the physiological enhancements translated directly into agronomic gains. Transgenic clones produced significantly higher tuber numbers and weights in G_1 and G_2. Enhanced photosynthetic capacity increased total photoassimilate supply, while *ClRan1* activity supported active cell division in developing tuber stolons and medullary tissues. In G_2, although total tuber number per plant slightly declined across all lines relative to earlier generations, total tuber yield remained high due to increased individual tuber size, illustrating the typical trade-off between tuber sink strength and tuber number in potato crop development (Sugiyono *et al*. 2021).

This study demonstrates the stable integration, transgenerational inheritance, and functional expression of *FBPase* and *ClRan1* transgenes in IPB CP1 potato across three consecutive generations (G_0, G_1, and G_2). Overexpression of both genes improved photosynthetic efficiency, stomatal conductance, plant height, and root length. Biomass allocation between roots and shoots remained balanced, maintaining a consistent root-to-shoot ratio, while primary photoassimilate partitioning was directed toward developing tubers. This preferential allocation produced significant improvements in tuber number and total tuber weight per plant in G_1 and G_2. Among all evaluated lines, clone C1FB4 demonstrated superior gene expression, physiological efficiency, and yield performance across all generations, highlighting its strong potential as an advanced transgenic line for national potato yield improvement.

Acknowledgements

This research was conducted without external financial support.

References

Akashi, K., Yoshimura, K., Kajikawa, M., Hanada, K., Kosaka, R., Kato, A., Katoh, A., Nanasato, Y., Tsujimoto, H., Yokota, A., 2016. Potential involvement of drought-induced Ran GTPase *CLRan1* in root growth enhancement in a xerophyte wild watermelon. *Biosci. Biotechnol. Biochem*. 80, 1907-1916. https://doi.org/10.1080/09168451.2016.1191328

Andrieu, A., Breitler, J.C., Siré, C., Meynard, D., Gantet, P., Guiderdoni, E., 2012. An in planta, *Agrobacterium*-mediated transient gene expression method for inducing gene silencing in rice (*Oryza sativa* L.) leaves. *Rice.* 5, 23. https://doi.org/10.1186/1939-8433-5-23

Baranauskaitė, L., Jurevičienė, D., 2021. Import risks of agricultural products in foreign trade. *Economies.* 9, 102. https://doi.org/10.3390/economies9030102

Clarke, P.R., Zhang, C., 2008. Spatial and temporal coordination of mitosis by Ran GTPase. *Nat. Rev. Mol. Cell Biol*. 9, 464-477. https://doi.org/10.1038/nrm2410

Daie, J., 1993. Cytosolic fructose-1,6-bisphosphatase: A key enzyme in the sucrose biosynthetic pathway. *Photosynth Res*. 38, 5-14. https://doi.org/10.1007/BF00015056

Deng, X., Shi, Z., Zeng, L., Lei, L., Xin, X., Pei, S., Xiao, W., 2021. Photosynthetic product allocations to the organs of *Pinus massoniana* are not affected by differences in synthesis or temporal variations in translocation rates. *Forests.* 12, 471. https://doi.org/10.3390/f12040471

Dodd, I.C., 2013. Abscisic acid and stomatal closure: a hydraulic conductance conundrum?. *New Phytologist* 197, 6-8. https://doi.org/10.1111/nph.12052

Eed, M., Alhussan, A.A., Qenawy, A.-S.T., Osman, A.M., Elshewey, A.M., Arnous, R., 2025. Potato consumption forecasting based on a hybrid stacked deep learning model. *Potato Res*. 68, 809-833. https://doi.org/10.1007/s11540-024-09764-7

Ezaki, K., Koga, H., Takeda-Kamiya, N., Toyooka, K., Higaki, T., Sakamoto, S., Tsukaya, H., 2024. Precocious cell differentiation occurs in proliferating cells in leaf primordia in *Arabidopsis angustifolia* 3 mutant. *Front. Plant Sci*. 15, 1322223. https://doi.org/10.3389/fpls.2024.1322223

Gizak, A., Duda, P., Wisniewski, J., Rakus, D., 2019. Fructose-1,6-bisphosphatase: From a glucose metabolism enzyme to multifaceted regulator of a cell fate. *Adv. Biol. Regul*. 72, 41-50. https://doi.org/10.1016/j.jbior.2019.03.001

Guo, R., Jin, Y., Liu, J., Yang, H., Cheng, L., Yu, B., 2025. Harnessing light quality for Potato production: red and blue light as key regulators of growth and yield. *Plants.* 14, 1039. https://doi.org/10.3390/plants14071039

Huang, L., Schiefelbein, J., 2015. Conserved gene expression programs in developing roots from diverse plants. *Plant Cell.* 27, 2119-2132. https://doi.org/10.1105/tpc.15.00328.

Hsu, P., Dubeaux, G., Takahashi, Y., Schroeder, J.I., 2021. Signaling mechanisms in abscisic acid-mediated stomatal closure. *Plant J*. 105, 307-321. https://doi.org/10.1111/tpj.15067

Kalendar, R., Orbovic, V., Egea-Cortines, M., Song, G., 2022. Editorial: Recent advances in plant genetic engineering and innovative applications. *Front. Plant Sci*. 13, 1045417. https://doi.org/10.3389/fpls.2022.1045417

Kamian, S., Ashoori, H., Vahidian, F., Davoudi, S., 2023. The relevance of common K-RAS gene mutations and K-RAS mRNA expression with clinicopathological findings and survival in breast cancer. *Asian Pac. J. Cancer Prev*. 24, 909-914. https://doi.org/10.31557/APJCP.2023.24.3.909

Livak, K.J., Schmittgen, T.D., 2001. Analysis of relative gene expression data using real-time quantitative PCR and the $2^{-\Delta\Delta CT}$ method. *Methods.* 25, 402-408. https://doi.org/10.1006/meth.2001.1262

Maulidiyah, R., Salam, M., Jamil, M.H., Tenriawaru, A.N., Rahmadanih, Heliawaty, Muslim, A.I., Bakheet Ali, H.N., Ridwan, M., 2025. Determinants of potato farming productivity and success: Factors and findings from the application of structural equation modeling. *Heliyon.* 11, e43026. https://doi.org/10.1016/j.heliyon.2025.e43026

Musawira., Tjahjoleksono, A., Hamim, H., Miftahudin, M., 2025. Drought tolerance in transgenic potato cultivar IPB CP1 expressing MmCuZn-SOD Gene. *HAYATI J. Biosci*. 32, 1377-1386. https://doi.org/10.4308/hjb.32.5.1377-1386

Niedbała, G., Niazian, M., Sabbatini, P., 2021. Modeling agrobacterium-mediated gene transformation of tobacco (*Nicotiana tabacum*)—A model plant for gene transformation studies. *Front. Plant Sci*. 12, 695110. https://doi.org/10.3389/fpls.2021.695110

Olivah, F.G., 2019. Genetic engineering of potato (*Solanum tuberosum* L.) cultivar IPB CP1 with *FBPase*/*ClRan1* genes mediated by *Agrobacterium tumefaciens* [Master's thesis]. Bogor, Indonesia: Institut Pertanian Bogor.

Paul, D., Das, D.N., Mondal, S., Gnanasekaran, S., Mor, A., Subramanya, K., 2022. Optimization of β-actin gene as a housekeeping gene for quantification of mRNA levels of target genes in buffalo endometrium. Indian *J. Physiol. Allied Sci*. 74, 7-11. https://doi.org/10.55184/ijpas.v74i04.65

Putra, F.H., Ishartati, E., Husain, S., 2019. Growth response of potato cuttings (*Solanum tuberosum* L.) granola Lembang varieties results of tissue culture to giving radix up with different segments. *JTCST.* 1, 44-51. https://doi.org/10.22219/jtcst.v1i2.9991

Ruan, W., Lai, M., 2007. Actin, a reliable marker of internal control?. *Clin. Chim. Acta* 385, 1-5. https://doi.org/10.1016/j.cca.2007.07.003

Song, G., Han, X., 2021. K-Domain technology: Constitutive expression of a blueberry keratin-like domain mimics expression of multiple MADS-Box genes in enhancing maize grain yield. *Front. Plant Sci*. 12, 664983. https://doi.org/10.3389/fpls.2021.664983

Sugiyono, S., Prayoga, L., Proklamasiningsih, E., Faozi, K., Prasetyo, R., 2021. The improvement of mini tuber production of Granola potato cultivar in aeroponics system. *Biosaintifika.* 13, 77-83. https://doi.org/10.15294/biosaintifika.v13i1.27714

Thanh, T., Chi, V.T.Q., Omar, H., Abdullah, M.P., Napis, S., 2012. Sequence analysis and potentials of the native RbcS Promoter in the development of an alternative eukaryotic expression system using green microalga Ankistrodesmus convolutus. *Int. J. Mol. Sci*. 13, 2676-2691. https://doi.org/10.3390/ijms13032676

Tian, C., Hua, X., Zhao, P., Li, C., Li, X., Liu, H., Liu, X., 2025. Genome-wide identification, evolution, and expression patterns of the Fructose-1,6-Bisphosphatase gene family in saccharum species. *Plants.* 14, 2433. https://doi.org/10.3390/plants14152433

Wei, Y.-S., Javed, T., Liu, T.-T., Ali, A., Gao, S.-J., 2025. Mechanisms of abscisic acid (ABA)-mediated plant defense responses: An updated review. *Plant Stress.* 15, 100724. https://doi.org/10.1016/j.stress.2024.100724

Xu, P., Cai, W., 2014. RAN1 is involved in plant cold resistance and development in rice (*Oryza sativa*). *J. Exp. Bot.* 65, 3277-3287. https://doi.org/10.1093/jxb/eru178

Yokota, A., Ashida, H., Akashi, K., Ushiyama, K., Shigeoka, S., discoverer; Nara Institute of Science and Technology. 2013 Jul 4. Method for production of stolon- forming plant having improved tuber production ability or stolon production ability compared with wild type, and stolon-forming plant produced by the method. United States Patent Application Publication US 20130174299A1.